

Fracture toughness of transverse cracks in graphite/epoxy laminates at cryogenic conditions

Sukjoo Choi¹, Bhavani V. Sankar^{*}

Department of Mechanical and Aerospace Engineering, University of Florida, 231 MAE-A Building, PO Box 116250, Gainesville, FL 32611, USA

Received 12 December 2005; received in revised form 12 March 2006; accepted 29 June 2006

Available online 14 September 2006

Abstract

Stress singularity of a transverse crack normal to ply-interface in a composite laminate is investigated using analytical and finite element methods. Four-point bending tests were performed on single-notch bend specimens of graphite/epoxy laminates containing a transverse crack perpendicular to the ply-interface. The experimentally determined fracture loads were applied to the finite element model to estimate the fracture toughness. The procedures were repeated for specimens under cryogenic conditions. Although the fracture loads varied with specimen thickness, the critical stress intensity factor was constant for all the specimens indicating that the measured fracture toughness can be used to predict delamination initiation from transverse cracks. For a given crack length and laminate configuration, the fracture load at cryogenic temperature was significantly lower. The results indicate that fracture toughness does not change significantly at cryogenic temperatures, but the thermal stresses play a major role in fracture and initiation of delaminations from transverse cracks. © 2006 Elsevier Ltd. All rights reserved.

Keywords: A. Polymer-matrix composites; B. Fracture toughness; C. Finite element analysis; D. Thermal analysis; Cryogenic temperature

1. Introduction

The next generation of space vehicles is supposed to provide a ten-fold reduction in the launch cost, from \$10,000 to \$1,000 per pound of payload. To reduce the launch cost, reducing the structural weight penalty of the space vehicle is necessary. Because of their high specific stiffness and strength fiber reinforced composites such as graphite/epoxy composites are candidate materials for cryogenic storage systems used in space vehicles, e.g., the liquid hydrogen (LH₂) tank.

A previous design of liquid hydrogen composite tank used composite sandwich structure made of graphite/epoxy composites and a honeycomb core. Typically a cryogenic composite tank is subjected to extreme temperature variation during and after re-entry into the atmosphere. During

the testing of a prototype composite tank microcracks developed in the inner facesheet of the sandwich structure at cryogenic conditions. Then the microcracks, which usually develop in the transverse plies, could become delaminations. This could have led to catastrophic failure of the sandwich structure [1]. The damage progression in laminated composites at cryogenic temperatures is illustrated in Fig. 1. At cryogenic temperatures, the microcracks initiate and propagate in laminated composites due to difference in thermal contraction between the fiber and matrix phases [2]. These microcracks propagate and result in transverse cracks. When the transverse crack develops further, the crack deflects through the interface between layers and delamination initiates. The delaminations connect the microcracks in adjacent layers and provide a leakage path for the cryogen. In the case of composite sandwich construction, debonding of the facesheet also develops. In a liquid hydrogen composite tank, this hydrogen leakage through the transverse cracks and delamination could cause the failure of the composite sandwich structures [1]. This failure motivates the present study on predicting the

^{*} Corresponding author. Tel.: +1 352 392 6749; fax: +1 352 392 7303.

E-mail address: sankar@ufl.edu (B.V. Sankar).

¹ Postdoctoral Associate.

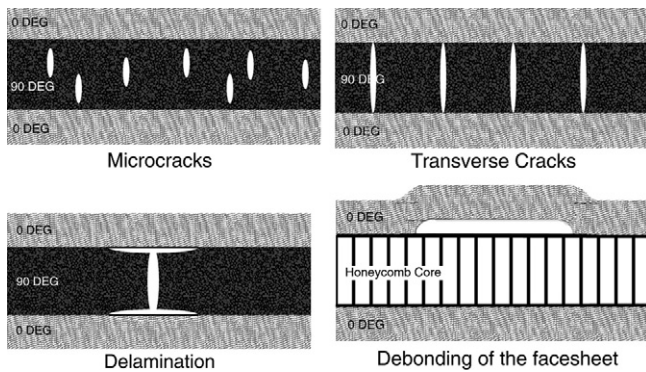


Fig. 1. Damage progression at cryogenic conditions.

fracture toughness of a transverse crack in composite laminates at cryogenic temperatures.

When a microcrack propagates normal to a ply-interface or causes a delamination between composite layers, its fracture toughness is governed by the stress singularity at the crack tip. Normal stresses at a crack tip are governed by stress singularity λ and stress intensity factor K_I as shown in Fig. 2. Williams [3] found the normal stresses ahead of a crack tip are proportional to $r^{-\lambda}$ ($0 < \text{Re}[\lambda] < 1$) where r is the distance from the crack tip. The stresses normal to the crack ahead of a crack tip can be expressed as $\sigma = K_I r^{-\lambda}$. The stress singularity of a transverse crack in laminated composites is governed by anisotropic material properties at the vicinity of a crack tip.

A microscopic image of cracks in a graphite/epoxy laminate is shown in Fig. 3. The 0° layer is stiffer than the 90°

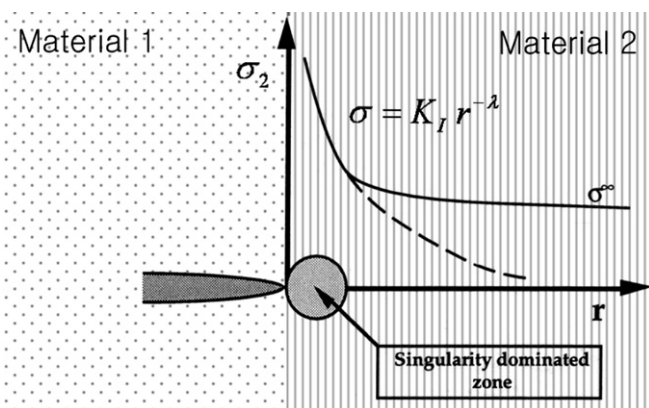


Fig. 2. Local stress field in the vicinity of a crack tip.

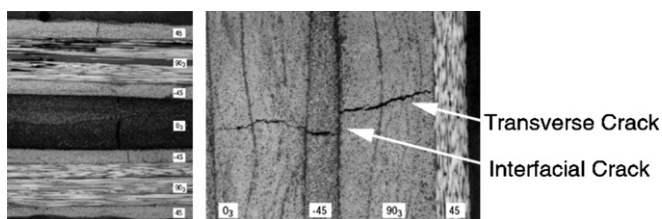


Fig. 3. SEM images of micro-crack propagation in composite laminates after thermo-mechanical cycles.

layer in the in-plane direction. When the transverse crack reaches a stiffer layer, it deflects into the ply-interface between layers and the interfacial crack or delamination continues to propagate. When the transverse crack reaches a softer layer, it penetrates into the next layer and continues to propagate until it reaches a stiffer layer [4]. In this study, conditions under which a transverse crack becomes a delamination are studied, and the fracture toughness of the transverse crack is quantified and measured.

Many researchers have studied the problem of stress singularity in bi-material systems, but not much work has been done on such crack propagation in fiber reinforced composite laminates. Zak and Williams [5] estimated the singularity for isotropic bi-material systems by solving a set of eigen functions developed by the continuity equations of normal and tangential stresses and displacements at the ply-interface. Ting and Chou [6] have developed methods to predict singularity at the free-edge of a ply-interface of laminated composites. The general equations of displacement and stresses are derived in terms of arbitrary constants. Stress singularity is determined when the boundary condition at a crack plane and the continuity equations at the ply-interface are satisfied. Later, Ting and Hoang [7] used this method to predict singularity of a transverse crack in laminated composites. Hutchinson and Suo [8] formulated a characteristic solution to predict stress singularity for isotropic bi-material systems in terms of Dundur's bi-material parameters α and β . Gupta et al. [4] formulated a characteristic solution to predict the singularity for anisotropic bi-materials in terms of bi-material parameters and individual material parameters. However, the characteristic equation is difficult to solve.

The behavior of the transverse fracture and ply delamination of composite laminates has been investigated by many researchers. Takeda and Ogihara [9] conducted experimental investigation to determine Young's modulus reduction and the mode II interlaminar fracture toughness K_{II} at room temperature and at 80°C . Wang and Karihaloo [10] investigated the transverse crack delamination of composite laminates in two cases. First, when the transverse crack resides within a layer, mode II fracture load F_{II} was determined using the analytical approach [11]. With the results, the layer orientation of a sample composite system was optimized to minimize interfacial stresses that cause mode II fracture. Second, when the transverse crack reaches the interface of an adjacent layer, the mode II stress singularities were determined for various composite materials with varying the ply orientation of the adjacent layer [11]. However, their study does not include the effects of temperature on transverse fracture. Petrossian and Wisnom [12] developed the finite element method using the interface elements to predict the failure loads of mode II delamination applying the plasticity theory.

The purpose of the study is to investigate the effect of cryogenic temperature on transverse crack propagation. The finite element model was developed to evaluate fracture toughness of the transverse crack in laminated

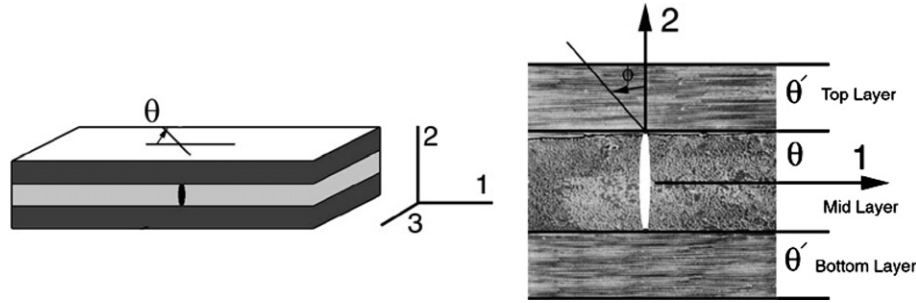


Fig. 4. Geometry of interfacial fracture specimens and a crack normal to laminate interface with different stacking sequence.

composites at room and cryogenic temperatures. Prior to the FE analysis, fracture loads were measured by experimental investigation at room and cryogenic temperatures. Comparison of fracture toughness values at room and cryogenic temperatures provide an understanding of the role of thermal stresses on the behavior of transverse cracks in laminated composites. The results from this study will be useful in understanding the effects of transverse cracks in composite storage systems at cryogenic temperatures.

2. Crack tip stress singularities for a crack normal to a ply-interface

The analytic approach is used to evaluate the singularity at the tip of a transverse crack in glass/epoxy and graphite/epoxy (IM7/977-2) composites with stacking sequence [0₃], [0/90/0] and [90/0/90] (see Fig. 4). In this study, stress singularity of a transverse crack in laminated composites is calculated using Ting’s methods [6,7], and finite element analysis is used to compute the crack tip stress fields in various laminated composite models.

The crack tip of the transverse crack is placed at the interface between top and mid-layers. The temperature dependent laminate properties used in this analysis are shown in Table 1 [2,13]. The singularities are compared

with the finite element results. The commercial computer program MATLAB[®] is used to solve the analytical equations. Finite element analysis is used not so much to verify the results from the analytical model but to determine the mesh refinement needed to obtain the proper singularity at the crack tip. In the finite element analysis the laminated composite beam was modeled using eight-node solid elements with 20 integration points. Glass/epoxy and graphite/epoxy (IM7/977-2) composites with stacking sequence [0₃], [0/90/0] and [90/0/90] are chosen to verify the stress singularity of the transverse crack. The ply thickness was taken as 2.2 mm. The length of the beam was 146 mm and the width 18.7 mm. An initial crack normal to a ply-interface is placed at the center of the beam subjected to tensile or bending loads (see Fig. 5). The region surrounding the crack tip was refined using 31,000 quadratic solid elements.

The composite beam model is subjected to four-point bending and tensile loading conditions as shown in Fig. 6. For the tensile case, uniform displacement in the in-plane direction is applied at the end of the bar. For bending cases, the beam is simply supported at 63.7 mm away from the crack. The top load is located at 19.5 mm away from the crack. The normal stresses ahead of the transverse crack tip are used to calculate the stress singularity.

A logarithmic plot of the normal stresses as a function of distance from the crack tip is used to determine the singularity in the FE model. The crack tip stress field is assumed to be of the form $\sigma = K_I \cdot r^{-\lambda}$, where $0 < \lambda < 1$. The stress singularity λ is estimated by calculating the slope of a logarithmic plot of normal stress as a function of distance r ahead of a crack tip.

The stress singularities determined from the finite element analyses are compared with the analytical results for various laminates in Tables 2 and 3. There seems to be a good agreement between the two sets of results. The

Table 1
Temperature dependent properties of carbon/epoxy laminates

	$T = 293 \text{ K}$	$T = 77 \text{ K}$
E_{11} (GPa)	159	160
E_{22}, E_{33} (GPa)	8.60	106
G_{12}, G_{13} (GPa)	3.95	5.35
G_{23} (GPa)	2.95	3.64
ν_{12}, ν_{13}	0.256	0.254
ν_{23}	0.446	0.448
α_{11} ($10^{-6}/^{\circ}\text{C}$)	-0.512	-0.621
α_{22}, α_{33} ($10^{-6}/^{\circ}\text{C}$)	16.3	14.1

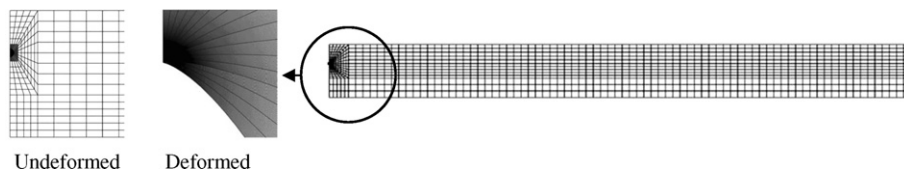


Fig. 5. Deformed geometry in the vicinity of a crack tip of the finite element model.

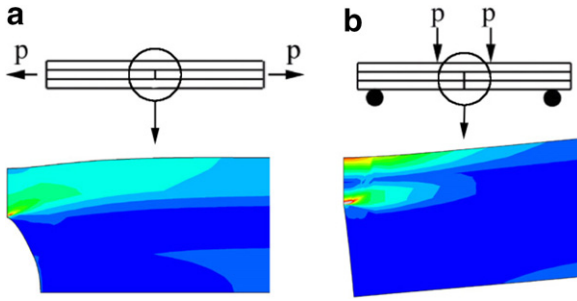


Fig. 6. Contour plots of stress distribution in a [0/90/0] composite laminate model at the crack tip under: (a) tensile load; (b) bending load.

Table 2
Singularity at the tip of a transverse crack in various E-glass/epoxy laminates

Layers	Analytical (Ting's)	FEM (ABAQUS)			
		Tensile	Difference from analytical (%)	Bending	Difference from analytical (%)
[0 ₃]	0.50	0.50	0.3	0.50	0.2
[0/90/0]	0.38	0.38	1.1	0.39	2.3
[90 ₃]	0.50	0.50	0.3	0.50	0.1
[90/0/90]	0.63	0.63	1.1	0.61	3.1

Table 3
Singularity at the tip of a transverse crack in various graphite/epoxy laminates

Layers	Analytical (Ting's)	FEM (ABAQUS)			
		Tensile	Error (%)	Bending	Error (%)
[0 ₃]	0.50	0.50	0.5	0.50	0.0
[0/90/0]	0.26	0.27	2.6	0.29	7.8
[90 ₃]	0.50	0.50	0.5	0.50	0.1
[90/0/90]	0.71	0.70	4.8	0.69	5.9

maximum difference between the two values is 7.8%. When the laminate orientation of the materials on both side of ply-interface are identical as in the case of unidirectional laminates, ([0₃] and [90₃]), the singularity $\lambda = 0.5$. When the laminate ahead of the crack tip is stiffer, as in [0/90/0] laminates, the stress singularity λ becomes less than 0.5, and it is greater than 0.5 when the crack is in the 0° ply touching the 0/90 interface as in [90/0/90] laminates. The results provide confidence in the accuracy of the finite element models in capturing the singularity for transverse cracks in a composite laminate. Then the FE model can be used to analyze several composite systems used in fracture tests.

3. Fracture toughness at room temperature

Four-point bending experiments were performed to determine the fracture loads of laminated beam specimens at room temperature as shown in Fig. 7. The four-point

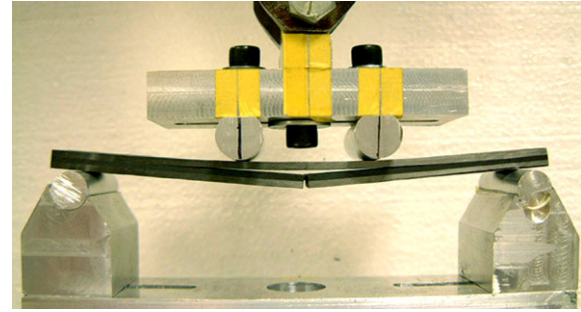


Fig. 7. Four-point bending test to determine the fracture load.

bending test has the advantages that it would yield more accurate and repeatable results as the transverse crack is in a region under constant bending moment without any transverse shear force. Even a small offset of the loading point with respect to the crack location will not significantly affect the results.

The proposed specimen has three layers of graphite/epoxy laminate with stacking sequence [0/90/0]. The top and bottom layers for all specimens have the same thickness of 2.4 mm and the mid-layer has various thicknesses, 1.8, 2.4 and 3.0 mm. The dimensions of specimens are listed in Table 4. An initial crack was created at the center of the specimen below the top layer. The notch was cut using a fine diamond saw, and then the razor blade was used to sharpen the crack tip. The initial crack tip is located in the mid-layer and below the ply-interface of the top layer. The specimen is simply supported at 63.7 mm away from the initial crack. The top loads are applied at a distance of 19.5 mm from the crack. The bending tests were conducted under displacement control in a material testing machine at a loading rate of 1.0 mm/min.

The load-deflection results of various specimens are shown in Fig. 8. The load increases linearly until the crack tip reaches the ply-interface of the top layer. After the interfacial fracture initiates, and as the crack propagates as a delamination, the load remains almost constant and the stiffness of the specimen reduces continuously. When the crack approaches the beam support, the energy release rate decreases and crack propagation stops. The load again increases linearly with deflection. The fracture loads F_c are measured at the instant when interfacial fracture initiates. The fracture loads for the three different specimens are listed in Table 5. One can note that the fracture load increases with the thickness of the middle 90° layer.

Table 4
Dimensions of specimens with various mid-ply thicknesses

[0/90/0]	Length (mm)	Width (mm)	Layer thickness	
			Top and bottom 0° layer (mm)	Mid 90° layer (mm)
Specimen 1	145.4	18.6	2.4	1.8
Specimen 2	146.2	18.7	2.4	2.4
Specimen 3	145.7	18.8	2.4	3.0

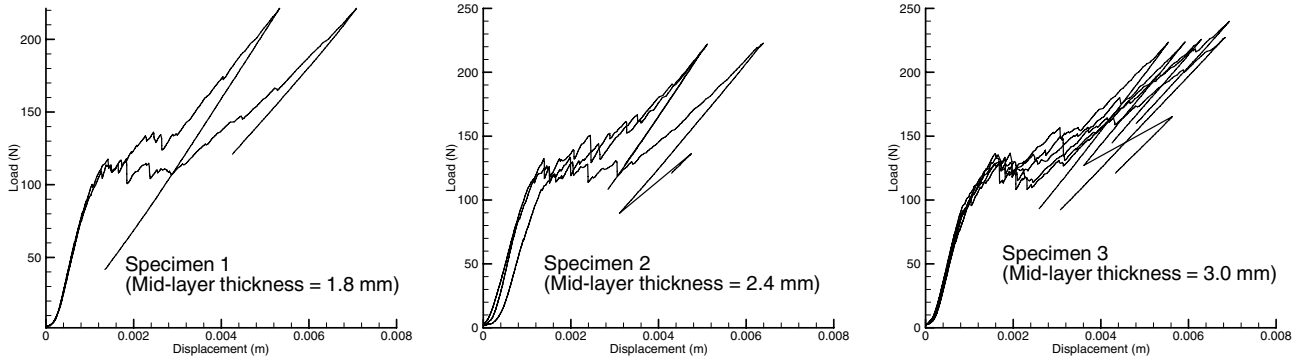


Fig. 8. Load–displacement curves of four-point bending tests at room temperature for various specimens with different mid-ply thicknesses.

Table 5
Fracture load (F_c) and fracture toughness (K_{Ic}) at room and cryogenic temperatures

[0/90/0]	Room temperature ($T = 300$ K)		Cryogenic temperature ($T = 77$ K)	
	F_c (N)	K_{Ic} (MPa·m ^{0.29})	F_c (N)	K_{Ic} (MPa·m ^{0.29})
Specimen 1	122	58.1	88.1	55.6
Specimen 2	127	57.9	81.5	58.1
Specimen 3	133	58.0	74.7	58.8
Average	127	58.0	81.4	57.5
Standard deviation (%)	4.3	0.2	8.2	2.9

Finite element analyses of the test specimens were performed to obtain the detailed stress field in the vicinity of the crack tip corresponding to the fracture loads. Due to symmetry one-half of the specimen is modeled. The laminate properties of graphite/epoxy given in Table 1 are used for the FE model. The composite laminates are in stress free condition at curing temperature ($T = 455$ K). Hence residual stresses exist even at room temperature ($T = 293$ K). A contour plot of the stress distribution is shown in Fig. 9. The fracture toughness K_{Ic} can be calculated in two ways. The first method is similar to the “stress matching” [14] as described by the equation below (see Fig. 10):

$$K_I = \lim_{r \rightarrow 0} \sigma(r)r^{\lambda} \quad (1)$$

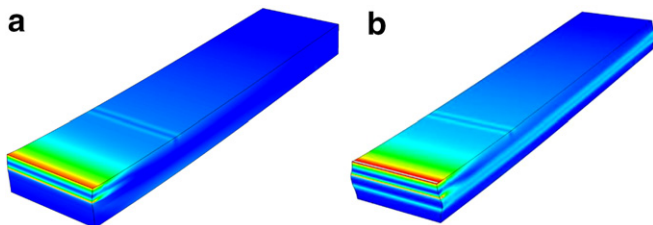


Fig. 9. Stress distribution for the four-point bending simulation at: (a) room temperature; (b) cryogenic temperature.

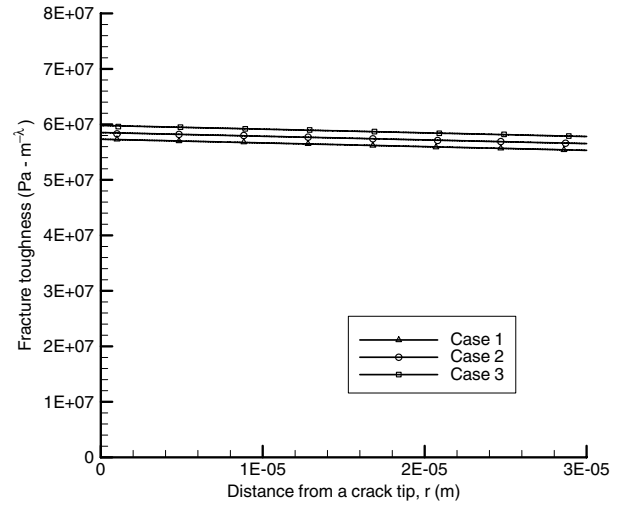


Fig. 10. Variation of $\bar{K} = \sigma r^\lambda$ with the distance from the crack tip, r at room temperature.

In the second method a logarithmic plot of σ vs. r is used to determine the best value of K by fitting (see Fig. 11):

$$\sigma(r) = K_I r^{-\lambda} \quad (2)$$

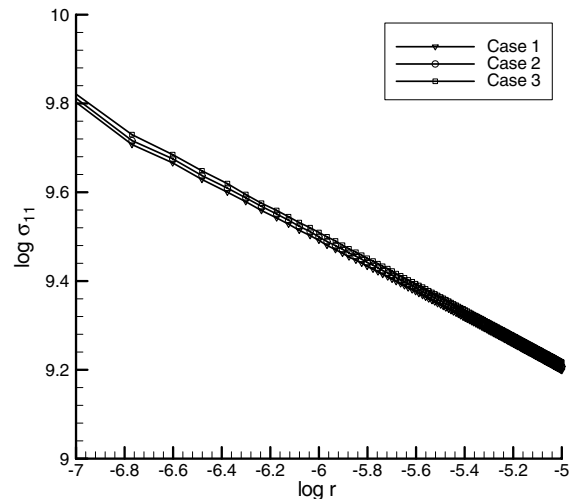


Fig. 11. Logarithmic plot of the stresses as a function of distance from the crack tip.

In both methods the singularity λ derived from the analytical method was used. The results for K from both methods were very close, and in this paper results from the stress matching method Eq. (1) are used.

From the results shown in Table 5, one can note that the increase in fracture load F_c is about 8% with 67% increase of mid-ply thickness. However the variation in the fracture toughness K_{Ic} is less than 1/2%. The results show that the fracture toughness is independent of the mid-ply thickness. Fracture toughness is only dependent on local material properties at the crack tip, but not on the global properties of the laminate system.

4. Fracture toughness at cryogenic temperatures

The effect of cryogenic temperature on fracture toughness is investigated by performing the fracture tests at liquid nitrogen temperature. Liquid nitrogen (LN_2) is used as the cryogenic refrigerant for several reasons. It is chemically inactive and non-toxic. Unlike hydrogen, nitrogen is safe to use in the laboratory. Liquid nitrogen is a colorless fluid like water.

The beam specimens were submerged initially in liquid nitrogen for about 5 min to reduce thermal gradients in the specimens (Fig. 12). The boiling temperature of LN_2 is 77 K. The specimen is placed in the cryogenic container with the liquid nitrogen. When the temperature of specimen reaches the boiling temperature, LN_2 boiling disappears. During this process, some specimens experienced delamination on the edge of mid-ply as shown in Fig. 13.

Finite element analysis was performed to investigate the edge delamination in the laminated specimens. The quarter region of the actual specimen was modeled using eight-

node 3-D solid elements. A contour plot of stresses in two-direction is shown in Fig. 14 when the FE model is subjected to cryogenic temperature ($T = 77$ K). The stresses in two-direction stay constant in 80% of the width and increases sharply near the edge as shown in Fig. 14. The sudden temperature decrease can be a reason for the edge delamination. Since graphite/epoxy composite has negative longitudinal CTE in the one-direction (see Table 1), the mid-layer expands and the top and bottom layer shrinks at cryogenic temperature. Therefore, Mode I fracture behavior can be expected at the edge. The result indicates that the edge delamination is not too deep to affect the experimental results for the fracture toughness of transverse cracks.

The four-point bending test fixture is placed in an insulated container and liquid nitrogen (LN_2) is filled up slowly. The LN_2 boiling disappears when the temperature of the test fixture becomes stable. During experiment, LN_2 is continuously added into the container so that specimen is completely submerged since LN_2 vaporizes due to the heat entering from the atmosphere. The four-point bending test is performed following the same procedures used for room temperature tests.

The load–displacement results are shown in Fig. 15. It is found that the fracture load decreases as the mid-ply thickness increases. Fracture load decreases by 15% with 67% increase in the mid-ply thickness as shown in Table 5. As shown will be later fracture load decrease may be due to thermal stresses in the vicinity of the crack tip at cryogenic temperature. Fracture toughness at cryogenic temperature is predicted using the finite element analysis. The temperature dependent laminate properties are used for the FE analysis at cryogenic temperature as shown in Table 1.



Fig. 12. Cryogenic experimental setup of the four-point bending test.

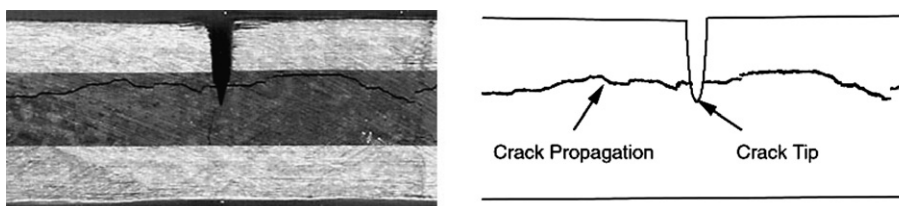


Fig. 13. Crack propagation in the 90° layer of a graphite/epoxy laminate at cryogenic temperature.

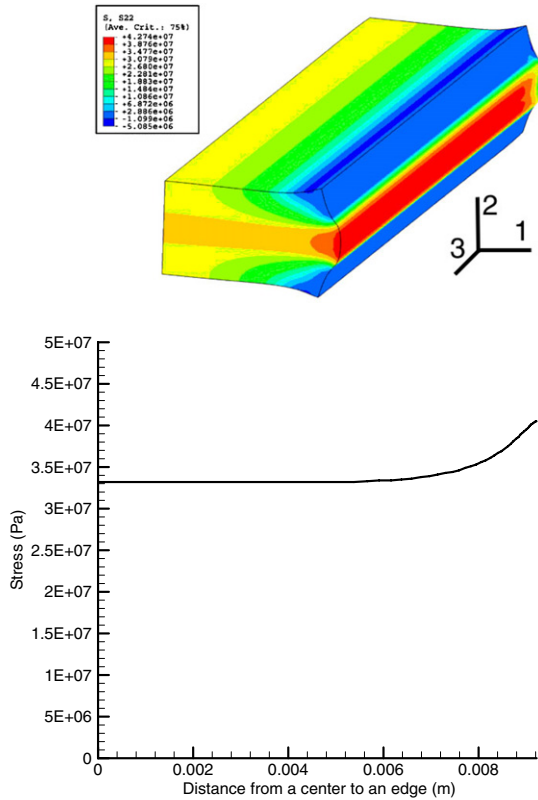


Fig. 14. Contour plot of stresses normal to ply direction near the free-edge in a graphite/epoxy laminate at cryogenic temperature.

The composite beam experiences temperature decrease from curing temperature ($T = 455$ K) to cryogenic temperature ($T = 77$ K). The contour plot of the stress distribution is shown in the Fig. 9. Fracture toughness is calculated following the same procedure as described in the previous section for room temperature tests. The variation of normal stresses with the distance from the crack tip is shown in Fig. 16. Although the fracture loads decreases by 15% with 67% increase in mid-ply thickness, fracture toughness increases by only 5%. The variation of fracture toughness between the three specimens tested at cryogenic temperature is insignificant. The result indicates that fracture toughness is not significantly affected by the

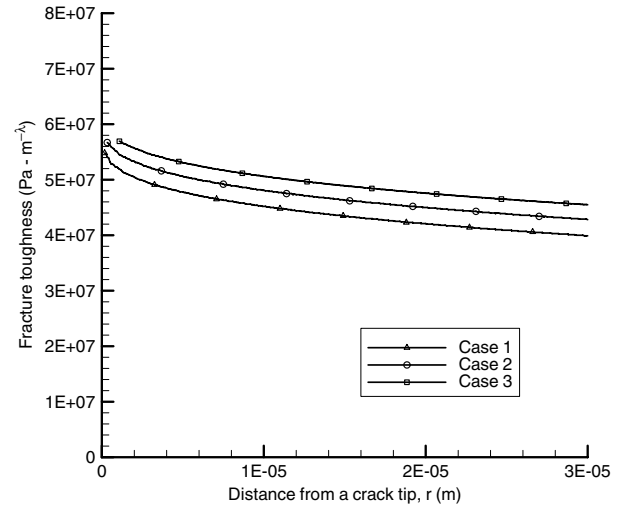


Fig. 16. Variation of $\bar{K} = \sigma r^{1/2}$ with the distance from the crack tip at cryogenic temperature.

cryogenic conditions. But, the fracture load significantly decreases due to thermal stresses present in the vicinity of the crack tip. At both room and cryogenic temperatures fracture toughness is estimated as 58 MPa. The result indicates fracture toughness is a characteristic property of the material system not governed by temperature changes.

It should be noted that the specimen dimensions and geometry are nominally the same for room temperature and cryogenic temperature tests. But, the fracture load is significantly lower at cryogenic temperature. However the fracture toughness, the critical stress intensity factor, seems to be the same. This is because there are significant thermal stresses at cryogenic temperature, which increases this stress intensity factor to a higher value. The same inference can also be made from the standard deviation of results shown in Table 5. The standard deviation for fracture loads is much higher than that for the fracture toughness at both room temperature and cryogenic temperature. Another observation is that the standard deviation of fracture toughness at cryogenic temperature is higher than that for room temperature tests indicating that it is difficult to obtain repeatable measurements under cryogenic

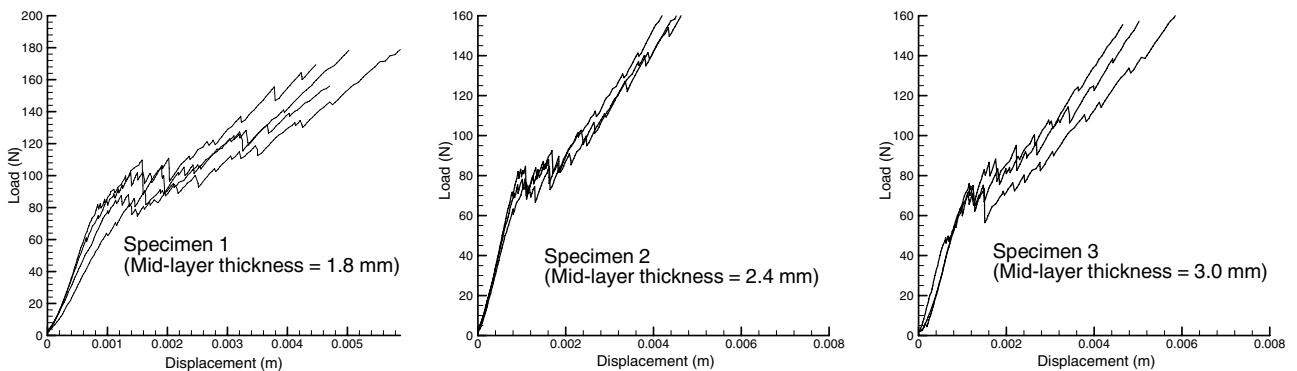


Fig. 15. Load–displacement curves from four-point bending tests at cryogenic temperature for various specimens with different mid-ply thicknesses.

conditions, and the test methods for cryogenic measurements need to be improved.

5. Conclusions

The stress singularity at the tip of a transverse crack touching a ply-interface in graphite/epoxy laminates was determined using an analytical procedure. The results were also verified by performing a finite element analysis of four-point bending and uniaxial tensile specimens containing a transverse crack. The results also provided confidence in the accuracy of the finite element models in capturing the singularity accurately. Fracture tests were performed using single edge notch bend specimens under four-point bending. The fracture load, the load at which delamination initiated from the transverse crack, was input in the FE model to determine the stress intensity factor and hence the fracture toughness. The temperature dependent properties were used for the analysis at room and cryogenic temperatures. The specimen is assumed to be in stress free condition at curing temperature. The experiments were repeated for various crack lengths and it was found that the fracture toughness was same for all specimens. The fracture tests were performed under cryogenic conditions by immersing the specimens in liquid nitrogen. The specimens failed at a much lower load compared to the room temperature tests. However, the results from the FE analysis showed that the fracture toughness was same as that at room temperature. The thermal stresses in the vicinity of the crack tip contributed to the increase in stress intensity factor causing the specimens to fracture at a lower load compared to room temperature tests. The results from this study will be useful in the design of composite storage systems for cryogenic applications.

Acknowledgements

The authors gratefully acknowledge the technical and financial support of NASA Glenn Research Center (NAG3-2750) and NASA Kennedy Space Center under

the Hydrogen Research and Education program. Partial support was provided by the CUIP (URETI) Program sponsored by NASA under NCC3-994, managed by NASA Glenn Research Center.

References

- [1] NASA. Final report of the X-33 liquid hydrogen tank test investigation team, George C. Marshall Space Flight center, Huntsville, AL, NASA Report, May 2000.
- [2] Choi S, Sankar BV. A micromechanics method to predict the micro-cracking of the LH₂ composite tank at cryogenic temperature. In: Proceedings of the fifth international congress on thermal stresses and related topics, Blacksburg, VA, June 2003. p. WM441–444.
- [3] Willams ML. On the stress distribution at the base of a stationary crack. *J Appl Mech* 1957;24:109–14.
- [4] Gupta V, Argon AS, Suo Z. Crack deflection at an interface between two orthotropic media. *J Appl Mech* 1992;59(June):79–87.
- [5] Zak AK, Williams ML. Crack point singularities at a bi-material interface. *ASME J Appl Mech* 1963;30:142–3.
- [6] Ting TCT, Chou SC. Stress singularities in laminated composites. fracture of composite materials. In: Proceedings of the second USA–USSR Symposium, Lehigh University, Bethlehem, PA, March 9–12, 1981;265–277.
- [7] Ting TCT, Hoang PH. Singularities at the tip of a crack normal to the interface of an anisotropic layered composite. *Int J Solids and Struc* 1984;20(5):439–54.
- [8] Hutchinson JW, Suo Z. Mixed mode cracking in layered materials. *Adv Appl Mech* 1991;29:63–191.
- [9] Takeda N, Ogihara S. Initiation and growth of delamination from the tips of transverse cracks in CFRP cross-ply laminates. *Compos Sci Technol* 1994;52:309–18.
- [10] Wang J, Karihaloo BL. Matrix crack-induced delamination in composite laminates under transverse loading. *Compos Struct* 1997;38:661–6.
- [11] Wang J, Karihaloo BL. Mode II and mode III stress singularities and intensities at a crack tip terminating on a transversely isotropic-orthotropic bi-material interface. In: Proceedings of the Royal Society of London 1994;A444.
- [12] Petrossian Z, Wisnom MR. Prediction of delamination initiation and growth from discontinuous plies using interface elements. *Compos Part A* 1998;29:503–15.
- [13] Agarwal B, Broutman L. Analysis and Performance of Fiber Composites. 2nd ed. New York: John Wiley and Sons Inc.; 1990.
- [14] Anderson TL. Fracture Mechanics, Fundamentals and Applications. 2nd ed. Boca Raton: CRC Press LLC; 1994.